

# Synthesis of calcium copper titanate ceramics via the molten salts method

Ke-pi Chen <sup>a,\*</sup>, Xiao-wen Zhang <sup>b</sup>

<sup>a</sup> Key Laboratory of Condition Monitoring and Control for Power Plant Equipment (North China Electric Power University),  
Ministry of Education, Beijing 102206, PR China

<sup>b</sup> State Key Laboratory of New Ceramics and Fine Processing, Tsinghua University, Beijing 100084, PR China

Received 10 June 2009; received in revised form 10 December 2009; accepted 2 February 2010

Available online 9 March 2010

## Abstract

$\text{CaCu}_3\text{Ti}_4\text{O}_{12}$  has a giant dielectric constant of up to  $10^4$  at room temperature and has great potential for various technological applications. In this work,  $\text{CaCu}_3\text{Ti}_4\text{O}_{12}$  ceramic powder was synthesized by heating a stoichiometric amount of  $\text{CaCO}_3$ ,  $\text{CuO}$  and  $\text{TiO}_2$  in molten  $\text{NaCl-KCl}$  and  $\text{Na}_2\text{SO}_4\text{-K}_2\text{SO}_4$ , respectively. The synthesis temperature was decreased from  $1000^\circ\text{C}$  (required by conventional solid-state reactions) to  $750^\circ\text{C}$  for  $\text{NaCl-KCl}$  or to  $850^\circ\text{C}$  for  $\text{Na}_2\text{SO}_4\text{-K}_2\text{SO}_4$ . The flux type has a larger influence on the phase compositions and morphology of the resultant powders than the synthesis temperature does. The dielectric constant of the resulting ceramics is more than  $10^4$  over the wide frequency range from 100 Hz to 100 kHz. The dielectric loss tangent of the resulting ceramics is lower than 0.2 in the frequency range from 100 Hz to 100 kHz. The dielectric behavior of both samples is similar to the results obtained for  $\text{CaCu}_3\text{Ti}_4\text{O}_{12}$  ceramics that were synthesized by the sol-gel method. © 2010 Elsevier Ltd and Techna Group S.r.l. All rights reserved.

**Keywords:** A. Powders; chemical preparation; C. Dielectric properties; D. Perovskite

## 1. Introduction

Materials with a high dielectric constant are widely used in technological applications such as for cellular phones, global positioning systems, capacitors, resonators and filters. High dielectric constants allow for smaller capacitive components and thus smaller electronic devices [1]. Recently,  $\text{CaCu}_3\text{Ti}_4\text{O}_{12}$  (CCTO) has attracted a significant amount of attention as a non-ferroelectric and lead-free ceramic because of its high permittivity ( $10^4$ ) and its insignificant temperature dependence on permittivity over the wide temperature range from 100 K to 500 K [2,3]. Several models have been proposed to explain this dielectric behavior [4]. Sinclair and co-workers carried out impedance spectroscopy measurements to demonstrate that CCTO ceramics are electrically heterogeneous and consist of semiconducting grains with insulating grain boundaries and asserted that the giant dielectric phenomenon is caused by a

grain boundary internal barrier layer capacitance (IBLC) rather than an intrinsic property associated with the crystal structure [5,6]. To date, the IBLC explanation of the extrinsic mechanism is widely accepted [7–10].

Various methods have been developed for the preparation of CCTO ceramics. They are usually produced by conventional solid-state reactions (SSR) from metal oxides at high temperatures (typically  $1000^\circ\text{C}$  for 20 h) with several intermediate grindings [5,6]. This method is tedious with relatively long reaction times, high temperature conditions and may still result in unwanted phases because of limited atomic diffusion through micrometer-sized grains [5]. Synthesis techniques other than solid-state reactions have been reported recently. Hassini et al. prepared CCTO using an organic gel-assisted citrate process [11] and Jha et al. prepared CCTO using a polymeric citrate precursor route but these methods are still relatively complex and require long heat treatment times [12]. Liu et al. prepared CCTO by pyrolyzing an organic solution containing stoichiometric amounts of the required metal cations and this was done at a lower temperature using a shorter reaction time than the conventional solid-state reactions [13]. Jin et al. prepared nano-ultrafine CCTO powders using the sol-gel method and the citrate auto-ignition method [14].

\* Corresponding author at: School of Energy and Power Engineering, North China Electric Power University, Beijing 102206, PR China.  
Tel.: +86 10 61772352; fax: +86 10 61772536.

E-mail address: [ckp@ncepu.edu.cn](mailto:ckp@ncepu.edu.cn) (K.-p. Chen).

Molten salt synthesis (MSS) is a well established low temperature synthesis technique that has recently attracted an increasing amount of interest. It has been used to synthesize ceramic powders such as  $\text{Pb}(\text{Mg}_{1/3}\text{Nb}_{2/3})\text{O}_3$  [15],  $\text{Bi}_4\text{Ti}_3\text{O}_{12}$  [16],  $\text{LaAlO}_3$  [17] and  $\text{MgAl}_2\text{O}_4$  [18]. As far as we know the synthesis of CCTO powders by MSS has not been reported. In this study, the MSS method was applied to the synthesis of CCTO powder using  $\text{Na}_2\text{SO}_4$ – $\text{K}_2\text{SO}_4$  and  $\text{NaCl}$ – $\text{KCl}$  eutectic mixtures as the flux, respectively. The effects of processing factors such as heating temperature and salt type on the formation of CCTO were investigated.

## 2. Experimental procedure

Reagent grade or other  $\text{CaCO}_3$ ,  $\text{CuO}$  and  $\text{TiO}_2$  were used as starting materials. Salts used were  $\text{NaCl}$ ,  $\text{KCl}$ ,  $\text{Na}_2\text{SO}_4$  and  $\text{K}_2\text{SO}_4$ . In this study, a  $\text{NaCl}$ – $\text{KCl}$  salt with a 1:1 eutectic composition was used and its melting point was about 657 °C; a  $\text{Na}_2\text{SO}_4$ – $\text{K}_2\text{SO}_4$  salt with a 0.75:0.25 eutectic composition was also used and its melting point was about 832 °C. For synthesizing CCTO powders using MSS, the following procedure was used. Firstly, a stoichiometric composition of  $\text{CaCO}_3$ ,  $\text{CuO}$  and  $\text{TiO}_2$  was ball-milled in acetone for 4 h in a polyethylene bottle using agate balls. And then the mixed powder was combined with  $\text{NaCl}$ – $\text{KCl}$  or  $\text{Na}_2\text{SO}_4$ – $\text{K}_2\text{SO}_4$  salt in a 1:1 salt/oxides weight ratio, respectively. Thirdly, mixtures were heated in a high purity alumina crucible for 2 h at a temperature between 750 °C and 1000 °C. At last, after cooling to room temperature, the reacted mass was washed for 2 h in hot deionized water to remove the salts. This washing process was

repeated about 20 times. The resultant powders were oven-dried at 105 °C for 4 h before characterization. The powders synthesized from  $\text{NaCl}$ – $\text{KCl}$  salt or  $\text{Na}_2\text{SO}_4$ – $\text{K}_2\text{SO}_4$  salt were designated as MSSA and MSSB, respectively. For preparing CCTO ceramics, the powders synthesized at 850 °C were used. The two kinds of powders were pressed in a 13-mm-diameter steel die. And then the pressed pellets were sintered at 1060 °C in air for 4 h and then furnace-cooled to room temperature.

Phases in the resultant powders and ceramics were identified by X-ray diffractometry (XRD, X'Pert Pro 2004, Panalytical, Netherlands). Patterns were recorded at 40 mA and 40 kV using  $\text{Cu K}\alpha$  radiation ( $\lambda = 1.54178 \text{ \AA}$ ). The scan rate ( $2\theta$ ) was 3°/min at a step size of 0.02°. ICDD cards were used to identify the phases present and they were 36-1451 ( $\text{CaCu}_3\text{Ti}_4\text{O}_{12}$ ), 10-173 ( $\text{CuO}$ ) and 5-669 ( $\text{CaTiO}_3$ ). The morphology of the as-washed powder was observed using scanning electron microscopy (SEM, JEOL, JSM6490LV, Japan). And the surface morphology of CCTO ceramics as-sintered was observed using scanning electron microscopy (SEM, JEOL, JSM6490LV, Japan) too.

For dielectric measurements, Ag electrodes were screen printed with Ag paste on both sides of the pellets and heat treated at 550 °C for 0.5 h. The frequency dependence of the dielectric constant was measured using a precision impedance Analyzer (Model HP4294A, Agilent Technologies, Singapore) over a frequency range from 40 Hz to 1 MHz.

## 3. Results and discussion

Fig. 1 shows XRD patterns of the powders obtained after water washing the reacted masses of stoichiometric  $\text{CaCO}_3$ ,

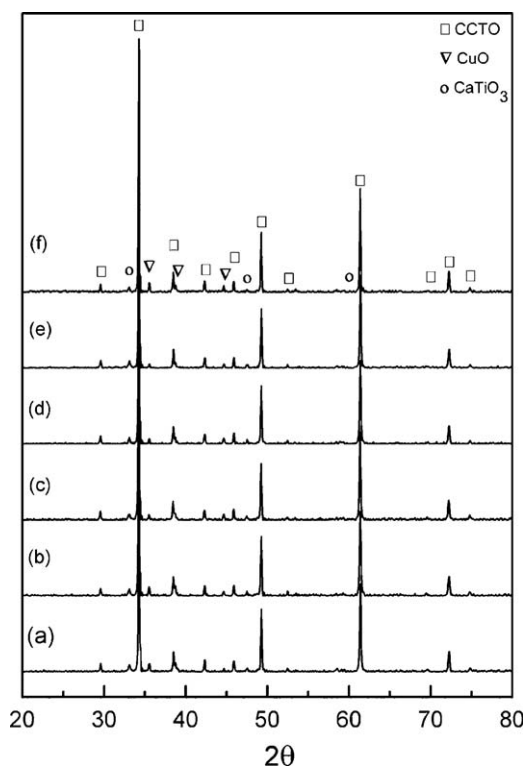


Fig. 1. X-ray diffraction patterns of the CCTO powder heated in  $\text{NaCl}$ – $\text{KCl}$  for 2 h at (a) 750 °C, (b) 800 °C, (c) 850 °C, (d) 900 °C, (e) 950 °C, and (f) 1000 °C.

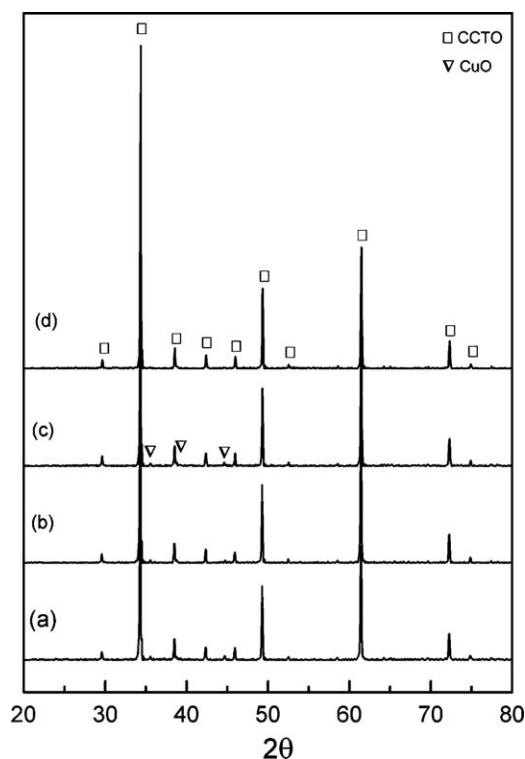


Fig. 2. X-ray diffraction patterns of the CCTO powder heated in  $\text{Na}_2\text{SO}_4$ – $\text{K}_2\text{SO}_4$  for 2 h at (a) 850 °C, (b) 900 °C, (c) 950 °C, and (d) 1000 °C.

CuO and  $\text{TiO}_2$  in NaCl–KCl salts. After heat treatment at 750 °C for 2 h, CCTO was the main phase with a small amount of CuO and  $\text{CaTiO}_3$ . This result indicates that CCTO formed below 750 °C when using the NaCl–KCl salt. The content of CCTO was almost constant as the temperature was increased from 750 °C to 1000 °C. Even when the temperature was increased to 1000 °C, peaks of CuO and  $\text{CaTiO}_3$  were still present. This indicates that the synthesis temperature has little effect on the purity of CCTO between 750 °C and 1000 °C. In other words, CCTO of high purity could be synthesized in the NaCl–KCl salt at any temperature from 750 °C to 1000 °C. However, it is difficult to synthesize CCTO by conventional solid-state reactions at temperatures lower than 1000 °C because of low solid-state diffusion. The molten salt eutectic accelerates the kinetics at this low temperature and facilitates the formation of CCTO. This can be attributed to the enhanced diffusion coefficients of the molten chloride liquid phase compared with that in the solid state. Furthermore, we found that the FWHM (full width at half maximum) of the typical diffraction peaks (2 2 0) for all of the samples synthesized by different reaction temperatures have almost the same amount, i.e. the instrumental width 0.18°. It means although reaction temperature reduced to 850 °C, the crystalline states of the synthesized powders had been well grown and developed. This

result is supported by SEM observation as shown in Fig. 3 later. Increasing the reaction temperature would, therefore, have little effect on the formation and development of the CCTO phase. At 850 °C, the NaCl–KCl melts start to vaporize and small weight losses are evident. This behavior increased sharply at temperatures higher than 900 °C [19]. It is thus difficult to control the reaction at high synthesis temperatures.

XRD patterns of the CCTO powders that were prepared by the MSS process in the  $\text{Na}_2\text{SO}_4$ – $\text{K}_2\text{SO}_4$  salt at different reaction temperatures for 2 h are shown in Fig. 2(a)–(d). For the powder obtained at 850 °C, CCTO was the main phase and CuO was the major impurity (Fig. 2(a)). After the reaction at 850 °C or 950 °C, CuO was still present (Fig. 2(b) and (c)). For the reaction at 1000 °C, all the diffraction peaks were due to body cubic CCTO and no trace of other phases was detected (Fig. 2(d)). Comparing Fig. 2 with Fig. 1, it seems that  $\text{Na}_2\text{SO}_4$ – $\text{K}_2\text{SO}_4$  is more effective in forming CCTO powder than NaCl–KCl. This may be attributed to differences in the melting point, viscosity and solubility of oxides in molten salts of  $\text{Na}_2\text{SO}_4$ – $\text{K}_2\text{SO}_4$  and NaCl–KCl. Nevertheless, the exact formation mechanism in both molten salts is complex and further work is underway.

The evolution of microstructure and particle size in the  $\text{CaCu}_3\text{Ti}_4\text{O}_{12}$  products was observed using SEM. Fig. 3(a) shows a typical SEM image of CCTO that was synthesized at 850 °C in the NaCl–KCl molten salt. CCTO powders show regular polyhedral morphology with an average particle size of about 2  $\mu\text{m}$ . A typical SEM image of CCTO synthesized at 850 °C in  $\text{Na}_2\text{SO}_4$ – $\text{K}_2\text{SO}_4$  is shown in Fig. 3(b). CCTO particle

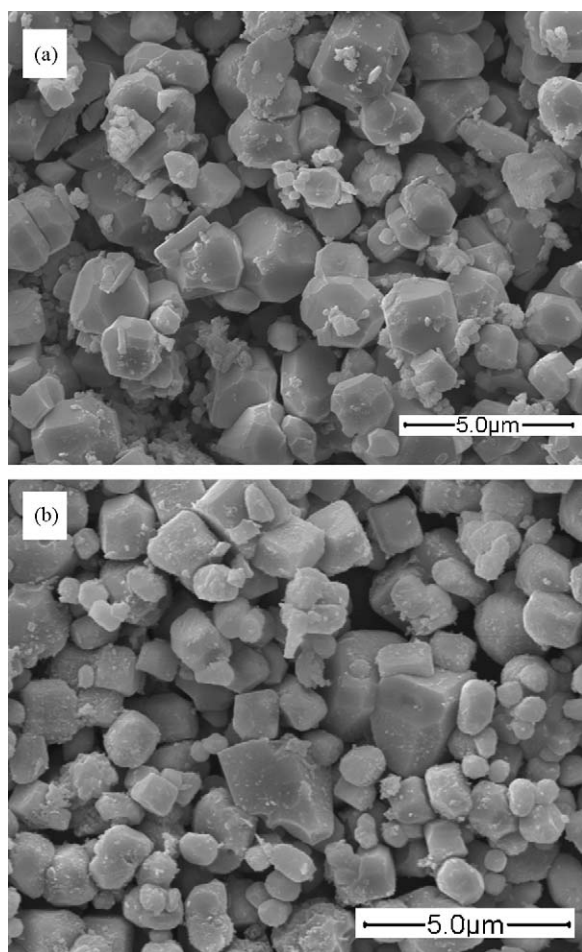


Fig. 3. Typical SEM images of the CCTO powder prepared at 850 °C (a) MSSA and (b) MSSB.

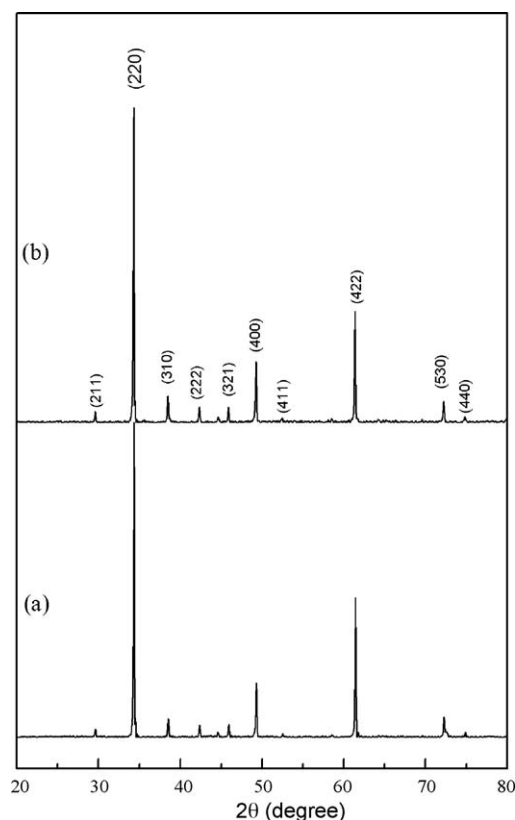


Fig. 4. X-ray diffraction of the CCTO ceramics (a) MSSA and (b) MSSB.

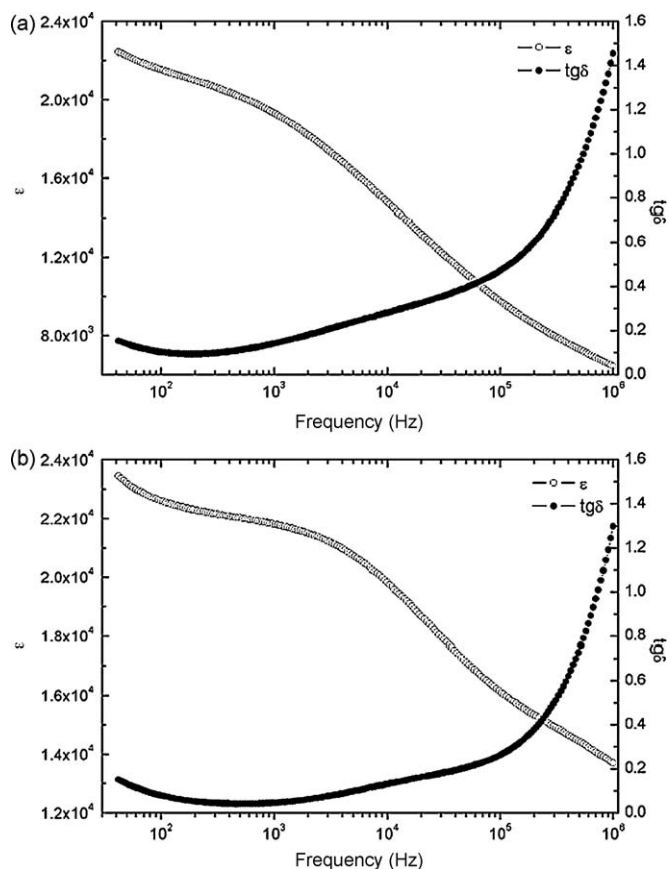


Fig. 5. Frequency dependence of the dielectric constant ( $\epsilon$ ) and the loss tangent ( $\tan \delta$ ) in the CCTO ceramics (a) MSSA and (b) MSSB.

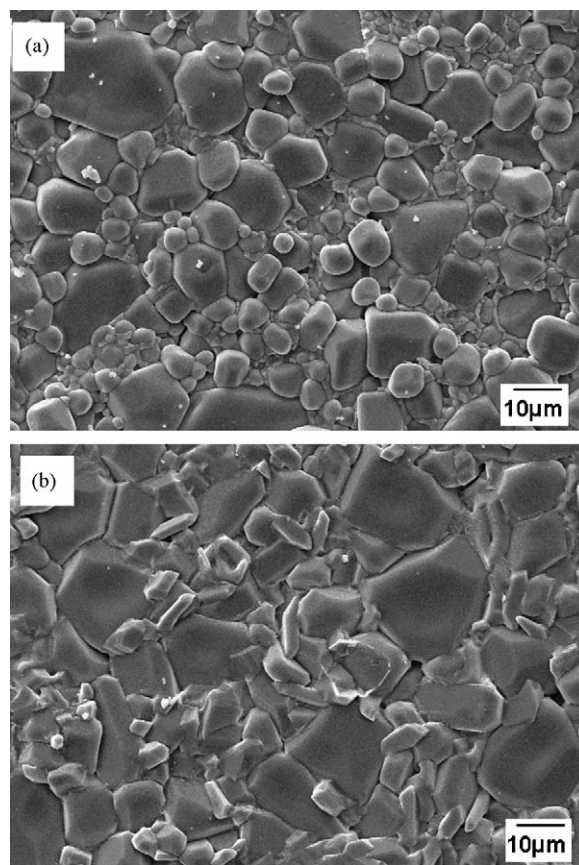


Fig. 6. SEM images of the surface morphology for the as-sintered CCTO ceramics (a) MSSA and (b) MSSB.

morphology, as shown in Fig. 3(b), is slightly different to that seen in Fig. 3(a) and this difference is attributed to differences in the melting point, viscosity and solubility of oxides in the molten salts of  $\text{Na}_2\text{SO}_4\text{--K}_2\text{SO}_4$  and  $\text{NaCl--KCl}$ . It is obvious that the molten salts play an important role in the development of CCTO particle morphology.

Fig. 4 shows the XRD patterns of CCTO ceramics that were sintered at  $1060^\circ\text{C}$  for 4 h. Both MSSA and MSSB ceramics show single-phase CCTO with all XRD peaks attributable to the cubic crystal structure and no traces of other phases were found. By comparison of Fig. 4 to Fig. 1(c) and Fig. 2(a), it can be deduced that CuO in powders synthesized by MSS is transformed into a liquid phase or that it reacts with  $\text{CaTiO}_3$  during sintering, which was also mentioned in the published paper by others [20]. The presence of a liquid phase is expected to have significant influence on the microstructure of CCTO ceramics.

The frequency dependence of the dielectric constant and the dielectric loss of the samples that were made from MSSA and MSSB at room temperature are shown in Fig. 5. The dielectric constant was found to be more than  $10^4$  over the wide frequency range from 100 Hz to 100 kHz. The dielectric loss tangent was lower than 0.2 in the range of frequency from 100 Hz to 100 kHz. The dielectric behavior of both samples was similar to that for CCTO ceramics produced by the sol–gel method and reported by Liu et al. [21]. We note that the variation in the

dielectric constant between the two samples synthesized from MSSA and MSSB powders does not necessarily mean that one synthesis technique is superior to the other because the dielectric constant of CCTO strongly depends on sample microstructure.

Representative SEM micrographs that were taken of as-sintered ceramic pellet surfaces are shown in Fig. 6 and these reveal that little difference exists in the microstructure of the powder from the different raw materials that were prepared using different molten salt systems. MSSA ceramics show a fine (average grain sizes of about  $5\ \mu\text{m}$ ) but dense uniform microstructure. MSSB ceramics show a fine (average grain sizes of about  $7\ \mu\text{m}$ ) and dense uniform microstructure too. No abnormal grains are found in the specimens of both the MSSA and MSSB ceramics. The only difference in microstructure between the two ceramics is the average grain size.

#### 4. Conclusions

Well-crystallized  $\text{CaCu}_3\text{Ti}_4\text{O}_{12}$  powders were successfully synthesized using  $\text{Na}_2\text{SO}_4\text{--K}_2\text{SO}_4$  and  $\text{NaCl--KCl}$  eutectic mixtures as the flux. The synthesis temperature was decreased from  $1000^\circ\text{C}$  (required for standard solid-state reactions) to  $750^\circ\text{C}$  for  $\text{NaCl--KCl}$  and  $850^\circ\text{C}$  for  $\text{Na}_2\text{SO}_4\text{--K}_2\text{SO}_4$ . The flux type has a larger influence on phase compositions and morphology of the resultant powders than the synthesis



temperature does. The dielectric constant of the resulting ceramics is more than  $10^4$  over the wide frequency range from 100 Hz to 100 kHz. The dielectric loss tangent of the resulting ceramics is lower than 0.2 in the frequency range from 100 Hz to 100 kHz. The dielectric behavior of both samples is similar to results obtained for  $\text{CaCu}_3\text{Ti}_4\text{O}_{12}$  ceramics that were synthesized by the sol–gel method.

## Acknowledgment

This work was partially supported by the Ministry of Science and Technology of China through a 973-Project under Grant No. 2006CB605105.

## References

- [1] B. Renner, P. Lunkenheimer, M. Schetter, A. Loidl, A. Reller, S.G. Ebbinghaus, Dielectric behavior of copper tantalum oxide, *J. Appl. Phys.* 96 (8) (2004) 4400–4404.
- [2] M.A. Subramanian, D. Li, N. Duan, B.A. Reisner, A.W. Sleight, High dielectric constant in  $\text{ACu}_3\text{Ti}_4\text{O}_{12}$  and  $\text{ACu}_3\text{Ti}_3\text{FeO}_{12}$  phases, *J. Solid State Chem.* 151 (2) (2000) 323–325.
- [3] C.C. Homes, T. Vogt, S.M. Shapiro, S. Wakimoto, A.P. Ramirez, Optical response of high-dielectric-constant perovskite-related oxide, *Science* 293 (5530) (2001) 673–676.
- [4] A.P. Ramirez, M.A. Subramanian, M. Gardel, G. Blumberg, D. Li, T. Vogt, S.M. Shapiro, Giant dielectric constant response in a copper-titanate, *Solid State Commun.* 115 (5) (2000) 217–220.
- [5] D.C. Sinclair, T.B. Adams, F.D. Morrison, A.R. West,  $\text{CaCu}_3\text{Ti}_4\text{O}_{12}$ : one-step internal barrier layer capacitor, *Appl. Phys. Lett.* 80 (12) (2002) 2153–2155.
- [6] T.B. Adams, D.C. Sinclair, A.R. West, Giant barrier layer capacitance effects in  $\text{CaCu}_3\text{Ti}_4\text{O}_{12}$  ceramics, *Adv. Mater.* 14 (18) (2002) 1321–1323.
- [7] L. Zhang, Z.J. Tang, Polaron relaxation and variable-range-hopping conductivity in the giant-dielectric-constant material  $\text{CaCu}_3\text{Ti}_4\text{O}_{12}$ , *Phys. Rev. B* 70 (17) (2004) 174306.
- [8] S.Y. Chung, I.D. Kim, S.J.L. Kang, Strong nonlinear current-voltage behaviour in perovskite-derivative calcium copper titanate, *Nat. Mater.* 3 (11) (2004) 774–778.
- [9] M.J. Pan, B.A. Bender, A bimodal grain size model for predicting the dielectric constant of calcium copper titanate ceramics, *J. Am. Ceram. Soc.* 88 (9) (2005) 2611–2614.
- [10] S.H. Hong, D.Y. Kim, H.M. Park, Y.M. Kim, Electric and dielectric properties of Nb-doped  $\text{CaCu}_3\text{Ti}_4\text{O}_{12}$  ceramics, *J. Am. Ceram. Soc.* 90 (7) (2007) 2118–2121.
- [11] A. Hassini, M. Gervais, J. Coulon, V.T. Phouc, F. Gervais, Synthesis of  $\text{Ca}_{0.25}\text{Cu}_{0.75}\text{TiO}_3$  and infrared characterization of role played by copper, *Mater. Sci. Eng. B* 87 (2) (2001) 164–168.
- [12] P. Jha, P. Arora, A.K. Ganguli, Polymeric citrate precursor route to the synthesis of the high dielectric constant oxide,  $\text{CaCu}_3\text{Ti}_4\text{O}_{12}$ , *Mater. Lett.* 57 (16–17) (2003) 2443–2446.
- [13] J.J. Liu, Y.C. Sui, C.G. Duan, W.N. Mei, R.W. Smith, J.R. Hardy,  $\text{CaCu}_3\text{Ti}_4\text{O}_{12}$ : low-temperature synthesis by pyrolysis of an organic solution, *Chem. Mater.* 18 (16) (2006) 3878–3882.
- [14] S.H. Jin, H.P. Xia, Y.P. Zhang, J.P. Guo, J. Xu, Synthesis of  $\text{CaCu}_3\text{Ti}_4\text{O}_{12}$  ceramic via a sol–gel method, *Mater. Lett.* 61 (6) (2007) 1404–1407.
- [15] K.H. Yoon, Y.S. Cho, D.H. Kang, Molten salt synthesis of lead-based relaxors, *J. Mater. Sci.* 33 (12) (1998) 2977–2984.
- [16] H. Hao, H.X. Liu, Y. Liu, M.H. Cao, S.X. Ouyang, Lead-free  $\text{SrBi}_4\text{Ti}_4\text{O}_{15}$  and  $\text{Bi}_4\text{Ti}_3\text{O}_{12}$  material fabrication using the microwave-assisted molten salt synthesis method, *J. Am. Ceram. Soc.* 90 (5) (2007) 1659–1662.
- [17] Z.S. Li, S.W. Zhang, W.E. Lee, Molten salt synthesis of  $\text{LaAlO}_3$  powder at low temperatures, *J. Eur. Ceram. Soc.* 27 (10) (2007) 3201–3205.
- [18] S.W. Zhang, D.D. Jayaseelan, G. Bhattacharya, W.E. Lee, Molten salt synthesis of magnesium aluminate ( $\text{MgAl}_2\text{O}_4$ ) spinel powder, *J. Am. Ceram. Soc.* 89 (5) (2006) 1724–1726.
- [19] X.R. Xing, C.Y. Zhang, L.J. Qiao, G.R. Liu, Facile preparation of  $\text{ZnTiO}_3$  ceramic powders in sodium/potassium chloride melts, *J. Am. Ceram. Soc.* 89 (3) (2006) 1150–1152.
- [20] S. Guillemet-Fritsch, T. Lebey, M. Boulos, B. Durand, Dielectric properties of  $\text{CaCu}_3\text{Ti}_4\text{O}_{12}$  based multiphased ceramics, *J. Eur. Ceram. Soc.* 26 (7) (2006) 1245–1257.
- [21] L.J. Liu, H.Q. Fan, P.Y. Fang, L. Jin, Electrical heterogeneity in  $\text{CaCu}_3\text{Ti}_4\text{O}_{12}$  ceramics fabricated by sol–gel method, *Solid State Commun.* 142 (10) (2007) 573–576.